J. Fluid Mech. (1971), *vol.* 45, *part* 2, *pp.* 247–260
Printed in Great Britain

Steady flow in the region of closed streamlines in a cylindrical cavity

By J. L. DUDA AND J. S. VRENTAS
Process Fundamentals Research Laboratory, The Dow Chemical Company, Midland, Michigan

(Received 3 March 1970)

An analytical solution is developed to describe the steady, closed streamline velocity field within a cylindrical cavity with a uniformly translating wall at low Reynolds numbers. The solution has application for the case of two-phase flow in a tube where regions of fluid are segmented by a moving train of bubbles or plugs, such as in the pulmonary and peripheral capillaries of the body where segments of plasma are trapped between red blood cells. The mathematical approach presented in this study can in principle be useful in the analysis of a wide class of closed-streamline creeping-flow problems.

Introduction

Fluid motions with closed streamlines involve complex two- or three-dimensional recirculating flow patterns and constitute an important class of flow fields. Perhaps the most extensively studied case in this class is the fluid motion generated in a rectangular cavity either by the translation of one of the walls (Burggraf 1966) or by the flow of a fluid over an open end of the cavity (Weiss & Florsheim 1965). The behaviour of a fluid in a cavity or notch and its influence on heat or mass transport through the cavity are important in the modelling of certain types of heat and mass transfer equipment. In addition, the analysis of cavity flow is relevant in bearing and seal studies and in certain aerodynamic applications. A closely related problem is that of circulation induced in an enclosed basin by surface stress due to the wind blowing along the top of the basin (Bye 1966).

Although the rectangular cavity has been perhaps the most widely examined closed-streamline flow field, there are other practically important and theoretically interesting flow fields with closed streamlines. For example, the movement of fluid droplets through another fluid gives rise to circulation currents within the droplets, and the analysis of this closed-streamline flow field and its influence on mass transfer is of considerable practical importance (Johns & Beckmann 1966; Kronig & Brink 1950). In addition, natural convection in cavities or other enclosed spaces is an example of a closed-streamline flow field caused by an unstable distribution of body forces due to temperature or concentration gradients (Gill 1966; Wilkes & Churchill 1966). Closed-streamline flows can also occur in unconfined regions such as the recirculating eddies formed in the flow over solid bodies. In a certain Reynolds number range, these eddies become relatively steady, recirculating flows which are separated from the main flow field (Burggraf 1966). Finally, an interesting example of a closed streamline flow associated with hydrodynamic instability is the toroidal or Taylor vortex flow which can be generated in the annulus between rotating cylinders (Taylor 1923).

An important closed-streamline velocity field which has attracted considerable interest is the circulating flow that results when a train of bubbles or plugs passes through a tube. If the diameter of the plugs is effectively equal to the inside diameter of the tube, then the fluid is confined and circulates between two successive plugs. A co-ordinate frame fixed in space and one moving at the speed of the plugs are related by a Galilean transformation so that the flow field between two plugs is simply related to the fluid motion produced by the steady movement of the wall surrounding a stationary cylindrical cavity filled with fluid. A schematic representation of such a cylindrical cavity and the associated surfaces of constant stream function is presented in figure 1, plate 1. The movement of plugs through a pipe has been termed bolus flow (Prothero & Burton 1961), and the principal features of this flow can be deduced by examining a single stationary cylindrical cavity with a uniformly translating wall. In particular, it is of interest to deduce the fluid-mechanical features of such a flow as well as to determine the influence of the flow field on heat and mass transfer processes in the cavity.

Several recent experimental studies have been concerned with flows which closely resemble the flow in a cylindrical cavity with solid walls. Differences result either because the plugs or bubbles do not completely fill the pipe or because the boundary conditions are slightly changed as is the case when gas bubbles are used instead of solid plugs. Oliver and co-workers (1964, 1968*a*, *b*) experimentally investigated the pressure drop and heat transfer characteristics of the slug flow régime of two-phase pipe flow with segments of liquid moving down the pipe between slugs of gas. These studies indicate that the induced circulation can increase the heat transfer coefficient by more than a factor of two over that realized in single-phase, laminar pipe flow. The fluid-mechanical aspects of bolus flow can also be of some importance in the design of the pipeline transport of solids in the form of capsules (Figueiredo & Charles 1968). Recently, Johansson, Olgard & Jernqvist (1970) have demonstrated that the unique characteristics of this flow field coupled with the radial migration of particles can be exploited to separate and fractionate particles in a suspension. Perhaps the most significant occurrence of bolus flow is in the pulmonary and peripheral capillaries of the body where segments of plasma are trapped between red blood cells which must deform in order to enter the capillary. It has been suggested that the circulation induced by the plugs of red cells increases the rate of gaseous equilibration within the plasma. In a recent survey by Wingard (1969) the problem of mass transfer in capillaries through which deformable sweeper particles pass is listed as one of the important fundamental technical problems in bioengineering.

Prothero & Burton (1961, 1962) have investigated the significance of this induced circulation in relation to oxygen transfer in pulmonary capillaries by conducting thermal analogue experiments. Their experiments, which involved heat transfer to a fluid flowing in a tube while segmented by gas bubbles, qualitatively confirm the results of Oliver and co-workers (1964, 1968*a*, *b*), and in some cases bolus flow was observed to be about twice as effective in transferring heat as Poiseuille flow. Visual observations and photographs of dye traces by Prothero & Burton revealed closed flow circuits similar to those depicted in figure 1.

To our knowledge, there exist no analytical or even finite-difference solutions of the equations describing both momentum and heat or mass transfer in bolus flow. Consequently, in this paper, an analytical solution is developed to describe the steady, closed-streamline velocity field within a cylindrical cavity with a uniformly translating wall at low Reynolds numbers where the inertial terms in the equations of motion can be safely neglected. In a second paper, this calculated velocity field is introduced into the energy equation, and an analytical solution is obtained describing the nature of the heat transfer enhancement due to the circulating bolus flow field. There are two basic objectives of the present investigation. First of all, there is the elucidation of the principal characteristics of heat and momentum transport in a relatively important flow situation. Secondly, there is the presentation of techniques and the accompanying mathematical paraphernalia which, in principle, can be of use in obtaining solutions to the equations which describe many other closed-streamline flow fields.

The results and techniques presented in this study are specific for low Reynolds number flows, but, in reality, this restriction is not too severe. This régime is of particular importance in the case of plasma flow in small capillaries. In addition, the experimental studies and approximate solution of Weiss & Florsheim (1965) and the finite-difference solutions of Burggraf (1966) for square cavities suggest that the zero Reynolds number solution describes the basic features of the flow quite well for Reynolds numbers as high as 150. Finally, interesting features of closed-streamline flows, such as corner eddies, can be more easily examined by utilizing analytical rather than finite-difference or approximate solutions.

Four recent theoretical papers serve to complement the results of the present work. Lighthill (1968) investigated the flow of tightly fitting solid pellets along elastic tubes, providing an analysis of the hydrodynamics in the lubricating film between the pellets and the tube wall. Wang & Skalak (1969) analyzed the creeping flow of fluid through a cylindrical tube containing rigid, spherical particles for sphere diameter-tube diameter ratios as high as 0·9. Bugliarello & Hsiao (1967) and Lew & Fung (1969) have previously considered the fluid-mechanical problem investigated in this paper. The first pair of authors utilized a finite-difference approach to generate a solution to the equations of motion whereas Lew & Fung obtained an analytical solution. Both the method and form of the solution of Lew & Fung (which was published after the present study was essentially complete) are substantially different from those of this investigation. In addition, a different method was used to obtain the first members of the infinite set of coefficients of the eigenfunction expansion. Lew & Fung utilized a collocation method whereas, in this study, the series coefficients were basically calculated by the usual approach, which requires that the difference between a function and its series representation be minimized in a least-squares sense over a finite interval. Finally, quite curiously, Lew & Fung reported results only for the case where the radii of the disks which separate segments of fluid were only 0·9 of the tube radius. The axial velocity in the gap between a disk and the tube wall was left unspecified and the mean velocity of the fluid between two disks was, consequently, less than the velocity of the disks.

The present study is regarded as a significant advancement over the previous work for the following reasons. First of all, in general, analytical solutions are to be preferred over finite-difference solutions because they better elucidate the structure of the solution to a problem, because they are flexible enough to permit easy evaluation of the effect of the parameters of the problem on the solution, and because they are better suited for the detailed examination of specific regions of a flow field (for example, a vortex centre or a corner eddy). The finite-difference results of Bugliarello & Hsiao are not utilized since an analytical expression for the stream function is needed if an analytical solution to the heat transfer problem is to be obtained. Furthermore, the collocation method for determining the coefficients of the series representing a function over an interval is generally regarded and often shown to be the least sophisticated of the error distribution methods; in addition, it is also frequently sensitive to the choice of collocation points. These shortcomings are of importance in the present instance since the forms of the eigenfunctions both for this work and for that of Lew & Fung are such that satisfying one of the boundary conditions near the point where the tube wall and the solid plug meet is a matter of some delicacy. Conceivably, the inadequacy of the collocation method is one reason why Lew & Fung chose not to extend the solid plug to meet the tube wall. On the other hand, determination of the eigenfunction coefficients by minimization of the Hilbert norm yields, with a reasonable number of coefficients, a very satisfactory representation of a Neumann condition on the tube wall with a minimal effect of the Gibbs phenomenon.

Comparison of the axial velocity profiles from the two aforementioned studies shows substantial differences near the tube wall, a region where such differences can profoundly influence the rate of heat transfer. It is felt that utilization of the analytical solution for the velocity field obtained in this paper in the energy equation rather than application of the solution of Lew & Fung is justified since the present work describes a limiting physical situation whereas it is not clear that the work of Lew & Fung can be easily extended to depict this limit. Two other new results of this paper are the careful mathematical analysis of the infinite set of equations for the coefficients and the presentation of a solution for the case where the plugs separating the liquid segments consist of inviscid fluids rather than solids.

Finally, Lew & Fung express the opinion that the effect of convection on oxygen transfer through capillary blood vessels is negligibly small, apparently because the streamlines as viewed by an observer fixed with respect to a capillary appear to differ only slightly from those for Poiseuille flow. It is shown in the second paper that this conclusion is correct but the reasoning is not. Indeed, it is the small value of the Péclet number for blood flow in capillaries which leads to a disappointingly small mass transfer enhancement.

Formulation of problem

Consider the laminar, steady flow of an incompressible Newtonian fluid with constant viscosity in a cylindrical cavity of the type depicted in figure 1. In the absence of gravitational effects it is possible to assume symmetry in the azimuthal direction with the velocity component in this direction everywhere equal to zero. In the limit of very low Reynolds numbers, the flow field is described by the following set of equations written in terms of dimensionless variables:

$$0 = -\frac{1}{U_a^2 \rho}\frac{\partial p}{\partial r} + \frac{2}{R_e}\left(\frac{\partial^2 V}{\partial r^2} + \frac{1}{r}\frac{\partial V}{\partial r} - \frac{V}{r^2} + \frac{\partial^2 V}{\partial z^2}\right), \quad (1)$$

$$0 = -\frac{1}{U_a^2 \rho}\frac{\partial p}{\partial z} + \frac{2}{R_e}\left(\frac{\partial^2 U}{\partial r^2} + \frac{1}{r}\frac{\partial U}{\partial r} + \frac{\partial^2 U}{\partial z^2}\right), \quad (2)$$

$$\partial V/\partial r + V/r + \partial U/\partial z = 0, \quad (3)$$

$$U(0,r) = 0, \quad U(\beta, r) = 0, \quad U(z,1) = -1, \quad (4), (5), (6)$$

$$(\partial U/\partial r)_{r=0} = 0, \quad (7)$$

$$V(0,r) = V(\beta, r) = 0, \quad V(z,1) = V(z,0) = 0, \quad (8), (9)$$

where the dimensionless quantities are related to their dimensional counterparts in the following manner:

$$\text{axial velocity} \quad U = U^*/U_a; \qquad \text{radial velocity} \quad V = V^*/U_a, \quad (10)$$

where U_a is the velocity of the cavity wall, velocity of plugs in a pipe;

$$\text{axial distance} \quad z = z^*/R; \qquad \text{radial distance } r = r^*/R, \quad (11)$$

where R is the radius of the cavity and L the length, p is the pressure, ρ the density, μ the viscosity, β the aspect ratio L/R and R_e is the Reynolds number $2RU_a\rho/\mu$.

The above equations of motion can be modified in the usual way yielding the slow flow form of the vorticity diffusion equation

$$\frac{\partial^2 \omega}{\partial r^2} + \frac{1}{r}\frac{\partial \omega}{\partial r} - \frac{\omega}{r^2} + \frac{\partial^2 \omega}{\partial z^2} = 0 \quad (12)$$

for the only non-vanishing component of the vorticity vector

$$\omega = \partial V/\partial z - \partial U/\partial r. \quad (13)$$

Introduction of a dimensionless stream function satisfying (3) by the equations

$$U = -(1/r)\,\partial\psi/\partial r, \quad V = (1/r)\,\partial\psi/\partial z, \quad (14), (15)$$

and utilization of (12) and (13) yield the expanded form of the fourth-order partial differential equation describing the spatial variation of the stream function for this flow field:

$$E^2(E^2\psi) = \frac{\partial^4\psi}{\partial r^4} + 2\frac{\partial^4\psi}{\partial r^2\,\partial z^2} + \frac{\partial^4\psi}{\partial z^4} - \frac{2}{r}\frac{\partial^3\psi}{\partial r^3} - \frac{2}{r}\frac{\partial^3\psi}{\partial r\,\partial z^2} + \frac{3}{r^2}\frac{\partial^2\psi}{\partial r^2} - \frac{3}{r^3}\frac{\partial\psi}{\partial r} = 0, \quad (16)$$

E^2 being

$$\frac{\partial^2}{\partial r^2} - \frac{1}{r}\frac{\partial}{\partial r} + \frac{\partial^2}{\partial z^2}.$$

Equation (16) is very similar to the cylindrical co-ordinate form of the biharmonic equation, and techniques useful in obtaining solutions to the biharmonic equation can often also be applied in determining solutions to the fourth-order stream-function equation. Finally, the boundary conditions, (4)–(9), can be rewritten as

$$\psi = 0,\ (1/r)\,\partial\psi/\partial r = \partial^2\psi/\partial r^2 \quad \text{for} \quad r = 0,\ 0 < z < \beta, \tag{17}$$

$$\psi = 0, \qquad \partial\psi/\partial r = 1 \quad \text{for} \quad r = 1,\ 0 < z < \beta, \tag{18}$$

$$\psi = 0, \qquad \partial\psi/\partial z = 0 \quad \text{for} \quad z = 0,\ 0 < r < 1, \tag{19}$$

$$\psi = 0, \qquad \partial\psi/\partial z = 0 \quad \text{for} \quad z = \beta,\ 0 < r < 1. \tag{20}$$

Equations (16)–(20) represent a well-posed system of equations describing the spatial variation of the stream function. Once the expression for the stream function is determined, it is an easy matter to calculate the velocity, vorticity and pressure fields from (13)–(15), (1) and (2).

Solution of fourth-order stream-function equation

The cylindrical cavity flow problem is such that the normal derivatives of the stream function are expressed in terms of series of non-orthogonal functions on the boundaries of the cavity. Consequently, although the eigenfunctions of the fourth-order partial differential equation form a complete set, the fact that they lead to series expansions of functions on the boundaries which are not mutually orthogonal poses a basic difficulty in the computation of the coefficients of the eigenfunction series. Burggraf (1966), Pan & Acrivos (1967), and Weiss & Florsheim (1965) experienced a similar predicament in attempting to obtain exact solutions for the creeping-flow equations describing the circulation patterns in square and rectangular cavities. Burggraf and Pan & Acrivos resorted to finite-difference techniques to obtain solutions, and Weiss & Florsheim utilized a variational principle to generate an approximate analytical solution to the biharmonic equation. The elasticity literature is perhaps the richest source of methods of obtaining solutions to the biharmonic equation, and series expansions of non-orthogonal functions in the mathematical theory of elasticity have been handled by application of the theory of infinite systems of linear algebraic equations. Kantorovich & Krylov (1958) and Timoshenko & Woinowsky-Krieger (1959) give examples of such an approach in solving the biharmonic equation describing the spatial variation of the deflexion of thin plates. Another possible method of resolving the problem is an orthogonalization procedure (Morse & Feshbach 1953) which involves linearly combining functions from the complete set of non-orthogonal functions to form a new set of functions which is also complete and, in addition, orthogonal. In this paper, we deduce the proper form of the eigenfunctions and employ the theory of infinite systems of equations as outlined by Kantorovich & Krylov to produce an analytical solution of the slow flow equation for the cylindrical cavity.

From the form of the partial differential equation and the nature of the boundary conditions and from completeness considerations, it follows that a solution of (16) can be written in the following form:

$$\psi = \sum_{n=1}^{\infty} \hat{R}_n(r) \sin\frac{n\pi z}{\beta} + \sum_{n=1}^{\infty} rJ_1(a_n r)\, Z_n(z), \tag{21}$$

$$J_1(a_n) = 0, \tag{22}$$

where J_n is the Bessel function of first kind of order n. Substitution of (21) into (16) produces homogeneous, ordinary differential equations for the $\hat{R}_n$ and the Z_n whose solutions can be combined to give the following form of the eigenfunction expansion for the stream function:

$$\psi = \sum_{n=1}^{\infty} A_n F_n(r) \sin\frac{n\pi z}{\beta} + \sum_{n=1}^{\infty} G_n(z)\, r J_1(a_n r), \tag{23}$$

$$F_n(r) = \frac{r I_1(n\pi r/\beta)\, I_2(n\pi/\beta) - r^2 I_1(n\pi/\beta)\, I_2(n\pi r/\beta)}{I_2^2(n\pi/\beta)}, \tag{24}$$

$$G_n(z) = B_n[e^{a_n z} - e^{-a_n z} - (z/\beta)\, e^{a_n(2\beta - z)} + (z/\beta)\, e^{-a_n z}] + C_n[z\, e^{a_n z} - z\, e^{a_n(2\beta - z)}], \tag{25}$$

where I_n is the modified Bessel function of first kind of order n. The three infinite sets of coefficients, A_n, B_n and C_n, must be chosen so that the Neumann conditions on the boundary of the cylindrical domain are satisfied.

Utilization of appropriate Fourier sine and Fourier–Bessel expansions in the Neumann boundary conditions yields the following set of equations for the three infinite sets of eigenfunction coefficients:

$$B_m = -\frac{4a_m\beta\, e^{a_m\beta} \sum_{n=1}^{\infty} A_n Q_{nm}}{g_m} + \frac{2(1 - e^{2a_m\beta}) \sum_{n=1}^{\infty} A_n Q_{nm}(-1)^n}{g_m}, \tag{26}$$

$$C_m = \frac{(4a_m\beta\, e^{a_m\beta} - 2e^{a_m\beta} + 2e^{-a_m\beta}) \sum_{n=1}^{\infty} A_n Q_{nm}}{\beta g_m} - \frac{(4a_m\beta + 2 - 2\, e^{2a_m\beta}) \sum_{n=1}^{\infty} A_n Q_{nm}(-1)^n}{\beta g_m}, \tag{27}$$

$$c_m = a_m A_m + \sum_{n=1}^{\infty}\sum_{p=1}^{\infty} A_n T_{mnp} \quad (m = 1, 2, \ldots). \tag{28}$$

Definitions of the quantities in these equations are given in the appendix. It is clear that the difficult task in completing the analytical solution of the fourth-order stream function equation is the determination of the infinite set of A_n from (28). This calculation, which involves solution of a single infinite system of linear algebraic equations, is discussed in the next section.

Explicit expressions for the velocity, pressure, and vorticity distributions can be derived from (1), (2), (13)–(15), and (23); these results are not presented here since they are of secondary importance for our purposes. The pressure distribution is of course essential in determining the resistance to flow for a bolus flow situation such as the circulation of blood in capillaries (Prothero & Burton 1962). The vorticity distribution is useful in investigating the structure of viscous eddies (Burggraf 1966). Finally, the position of the vortex centre of the circulation pattern can be derived from the equations for the velocity components by setting $U = V = 0$.

Solution of infinite system of equations

Kantorovich & Krylov (1958) present a detailed discussion of the theory germane to the solution of an infinite system of equations for an infinite set of unknowns. They establish the necessary existence and uniqueness theorems and indicate a method of determining approximate values of the unknowns by means of a finite number of operations. The following three theorems, valid for a special class of infinite systems denoted as fully regular by these authors, will be useful in the present study:

THEOREM 1. *The solution of a fully regular system exists for any bounded set of free terms.*

THEOREM 2. *A fully regular system with bounded free terms always has a unique bounded solution, which may be found by the method of successive approximations starting from any bounded system of initial values.*

THEOREM 3. *The solution of a fully regular system with bounded free terms may be found by the method of reduction. The method of reduction involves the solution of finite systems derived from the infinite system by discarding all equations and unknowns beginning with a certain one. The solutions of such finite systems approach the solution of the infinite system as more equations and unknowns are retained. An infinite system of linear equations of the form*

$$x_i = \sum_{k=1}^{\infty} C_{ik} x_k + b_i \quad (i = 1, 2, \ldots) \tag{29}$$

is called a fully regular system with bounded free terms if

$$\sum_{k=1}^{\infty} |C_{ik}| \leqslant K_1 < 1 \quad (i = 1, 2, \ldots), \tag{30}$$

$$|b_i| \leqslant K_2, \tag{31}$$

where K_2 is a constant and K_1 is a constant number less than one.

It can be shown that, at least for the range of β values used here, (28) is a fully regular infinite system with bounded free terms. Therefore, by the above three theorems, we are assured of obtaining a unique, bounded solution by solving progressively bigger finite systems. In this manner, we can asymptotically approach the solution to the infinite system; in practice, we say that we have effectively attained this solution when the solution essentially stops changing as the size of the finite system grows. It can be shown that the even-numbered eigenfunction coefficients obey the relation

$$A_n = 0 \quad (n = 2, 4, \ldots), \tag{32}$$

so that only the odd-numbered equations must be considered in solving for the unknowns $A_1, A_3, \ldots$. Equation (32) is simply a consequence of the obvious symmetry of the flow field in the limit of low Reynolds numbers.

The first twenty eigenfunction coefficients for four values of β are recorded in table 1. In each case, these coefficients were determined by solving a finite system of 40 equations by the method of successive approximations. Further increase of the size of the finite system had negligible effect on the first twenty coefficients of each set. These twenty coefficients were adequate for accurate determination of the stream-function distribution.

	$\beta = 0{\cdot}5$	$\beta = 1{\cdot}0$	$\beta = 5{\cdot}0$	$\beta = 20{\cdot}0$
$-A_1$	$117{\cdot}980 \times 10^{-2}$	$68{\cdot}570 \times 10^{-2}$	$10{\cdot}375 \times 10^{-2}$	$2{\cdot}505 \times 10^{-2}$
$-A_3$	59·384	49·973	12·362	2·545
$-A_5$	37·958	34·349	13·623	2·618
$-A_7$	27·667	25·791	13·466	2·714
$-A_9$	21·668	20·528	12·559	2·821
$-A_{11}$	17·727	16·986	11·440	2·927
$-A_{13}$	14·977	14·447	10·455	3·021
$-A_{15}$	12·937	12·540	9·514	3·097
$-A_{17}$	11·363	11·056	8·690	3·151
$-A_{19}$	10·114	9·854	7·972	3·181
$-A_{21}$	9·100	8·890	7·347	3·190
$-A_{23}$	8·259	8·087	6·802	3·178
$-A_{25}$	7·552	7·408	6·322	3·150
$-A_{27}$	6·949	6·828	5·899	3·108
$-A_{29}$	6·429	6·326	5·523	3·055
$-A_{31}$	5·977	5·888	5·188	2·994
$-A_{33}$	5·580	5·503	4·887	2·928
$-A_{35}$	5·228	5·161	4·616	2·857
$-A_{37}$	4·915	4·857	4·371	2·785
$-A_{39}$	4·635	4·583	4·148	2·711

TABLE 1. Calculated eigenfunction coefficients

Results and discussion

Streamline patterns for cylindrical cavities for $\beta = 0{\cdot}5$, 1, and 5 are shown in figures 2–4. For $\beta = 0{\cdot}5$ there exists a two-cell recirculation pattern quite similar to the multicellular circulation patterns observed by Pan & Acrivos (1967) and Weiss & Florsheim (1965) for tall rectangular cavities. In fact, the second cell appears at approximately the same aspect ratio in all three studies. No corner eddies of the type discussed by Pan & Acrivos and Burggraf (1966) were detected in this study because the boundary conditions at the centreline of the cylindrical cavity are of course quite different than those at the solid bottom wall of the rectangular cavity.

As β becomes large, the streamlines in the centre of the cavity become essentially parallel to the cavity wall. Indeed, it follows from (23) and (28) that, as $\beta \to \infty$, the eigenfunction coefficients can be expressed as

$$A_n = -[1-(-1)^n]/4\beta \tag{33}$$

and the stream function is thus given by

$$\psi = \tfrac{1}{2}(r^4 - r^2). \tag{34}$$

Equation (34) is the relation for the stream function for laminar flow in a pipe expressed in terms of a velocity relative to a co-ordinate system moving with the average velocity of the fluid. It can be seen from figure 4 that, for values of β as low as five, the streamlines are effectively parallel for a good part of the region inside the cavity.

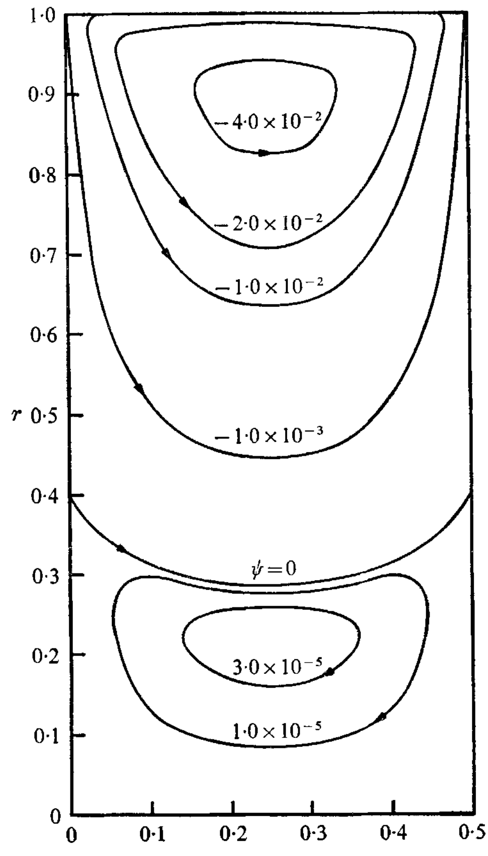

FIGURE 2. Streamline pattern for $\beta = 0{\cdot}5$ with no slip boundary condition.

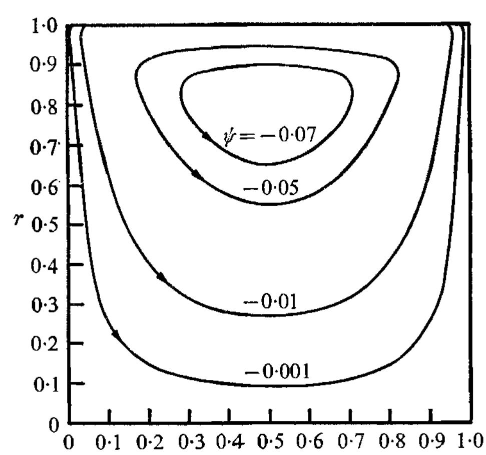

FIGURE 3. Streamline pattern for $\beta = 1$ with no slip boundary condition.

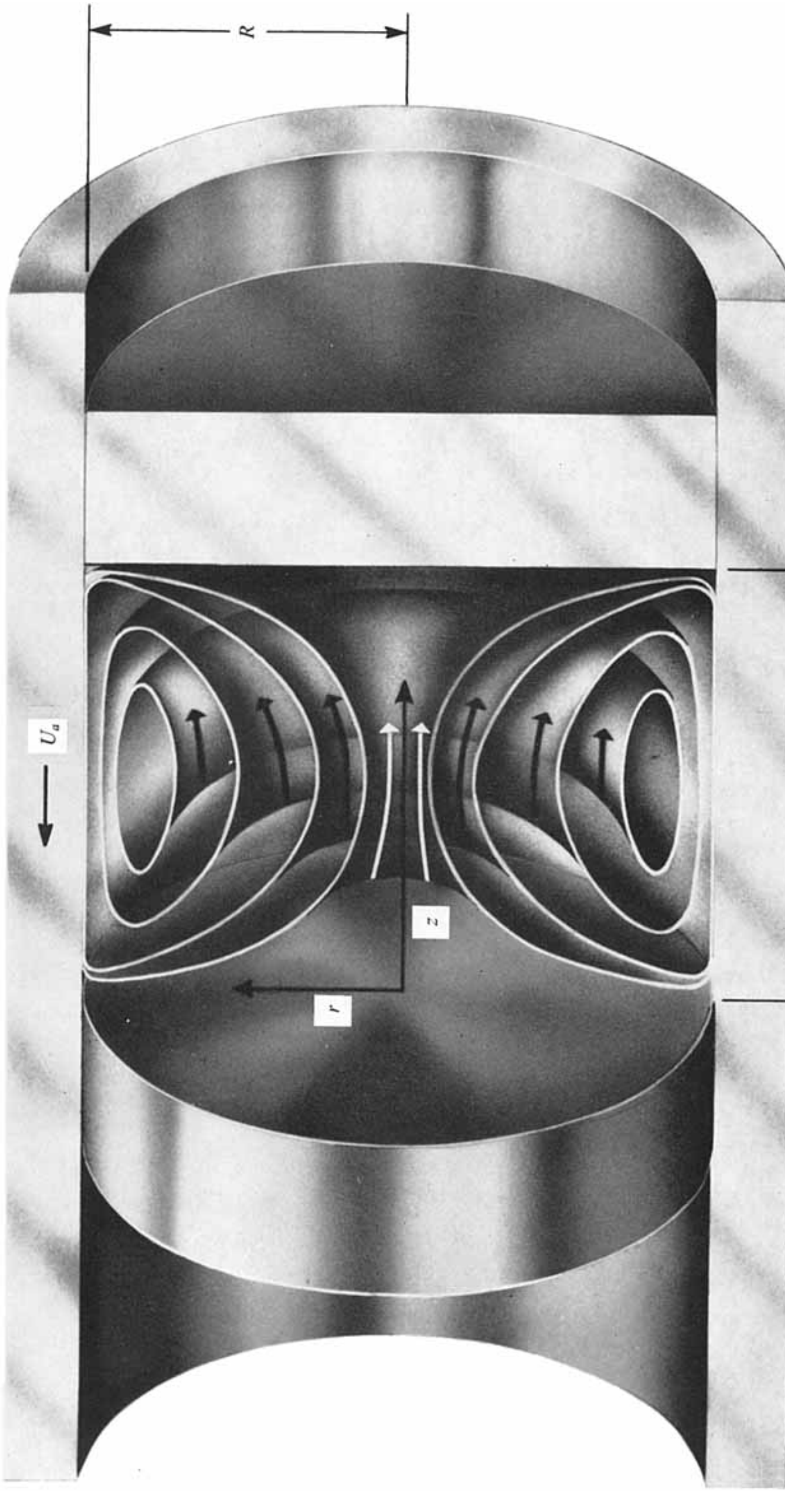

FIGURE 1. Schematic diagram of stream surfaces for flow in a cylindrical cavity.

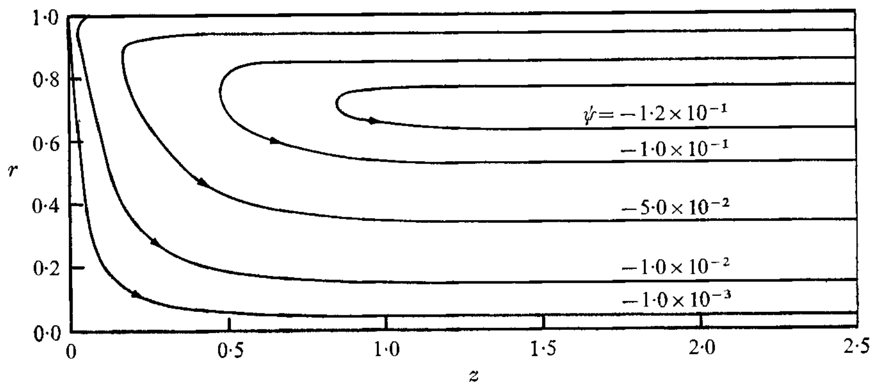

FIGURE 4. Streamline pattern for $\beta = 5$ with no slip boundary condition.

Locations of the vortex centres are presented in table 2. All of the cell centres are of course at $z = \frac{1}{2}\beta$ for the creeping-flow régime. It follows from (34) that the vortex centre for $\beta = \infty$ must occur at

$$r = \tfrac{1}{2}\sqrt{2}, \tag{35}$$

with

$$\psi = -\tfrac{1}{8}. \tag{36}$$

It is clear from table 2 that these limits are effectively realized for values of β as low as five.

β	First vortex r	First vortex ψ	Second vortex r	Second vortex ψ
	Solid plugs with no slip boundary condition			
0·5	0·888	$-4{\cdot}7 \times 10^{-2}$	0·212	$3{\cdot}8 \times 10^{-5}$
1·0	0·794	$-8{\cdot}6 \times 10^{-2}$	—	—
5·0	0·707	$-12{\cdot}5 \times 10^{-2}$	—	—
20·0	0·707	$-12{\cdot}5 \times 10^{-2}$	—	—
∞	0·707	$-12{\cdot}5 \times 10^{-2}$	—	—
	Inviscid gas plugs with no drag boundary condition			
0·5	0·845	$-6{\cdot}4 \times 10^{-2}$	—	—
1·0	0·752	$-10{\cdot}5 \times 10^{-2}$	—	—
∞	0·707	$-12{\cdot}5 \times 10^{-2}$	—	—

TABLE 2. Location of vortex centres

Other aspects of the flow field, such as vorticity and pressure distributions and velocity profiles, can be calculated from the above results, but they are not presented here because they are not of primary interest in the present work. The above results depict quantitatively the nature of the fluid motion in a cylindrical cavity for very low Reynolds numbers. In addition, a relatively simple approach is presented for obtaining analytical solutions to closed-streamline creeping-flow problems. The stream functions calculated in this paper are used in a second paper in the analysis of heat transfer to a cylindrical cavity with a uniformly translating wall.

Bolus flow is defined most generally (Prothero & Burton 1961) as the motion that results when a fluid element of one phase separates two elements of another phase as the train moves down a tube. Above, we have derived the velocity field for the special bolus flow motion that is caused by solid plugs flowing between elements of an incompressible fluid; in a stationary co-ordinate system, this flow field reduces to the cylindrical cavity problem with solid plane surfaces and a uniformly translating curved surface. The decision to concentrate on this particular physical situation was dictated primarily by three considerations. First of all, this representation appears to be a reasonable first approximation to blood flow through small capillaries. Secondly, the cylindrical cavity with solid walls is physically similar to the important rectangular cavity, and the basic method of solution used here should also be helpful in examining the fluid motion in the rectangular geometry. Finally, the no slip boundary condition at the surface of a solid plug is one limiting case of the interaction between the two phases flowing down the tube.

The other limiting case is that of an inviscid gas phase separating elements of a liquid phase. For this situation the boundary conditions at $z = 0$ and $z = \beta$ are modified in such a manner that the solution is significantly simpler than that presented above. If it is assumed that the diameter of the gas bubbles is effectively equal to the diameter of the tube and that the gas-liquid interface is not curved, it follows that the no drag condition can be written as

$$(\partial v/\partial z)_{z=0} = (\partial v/\partial z)_{z=\beta} = 0, \tag{37}$$

or, equivalently,

$$\partial^2\psi/\partial z^2 = 0 \quad \text{for} \quad z = 0, z = \beta, 0 < r < 1. \tag{38}$$

With this change in the set of boundary conditions presented earlier, the solution to (16) can be expressed in the following form:

$$\psi = \sum_{n=1}^{\infty} \hat{A}_n F_n(r) \sin\frac{n\pi z}{\beta}, \tag{39}$$

with the eigenfunction coefficients given by

$$\hat{A}_n = c_n/a_n. \tag{40}$$

It is clear that a considerable simplification in the form of the solution results by letting the viscous shear stresses vanish on the plugs surrounding the fluid. Bhattacharji & Savic (1965) derived an analytical solution, similar in some respects to (39), for the case of a gas piston driving a Newtonian fluid through a circular pipe. The extent of the fluid ahead of the piston was considered infinite. For this semi-infinite region, the eigenfunctions are necessarily in terms of a Fourier integral rather than a Fourier series and the eigenvalues form a continuous rather than a discrete spectrum.

Streamline patterns for the case of gas plugs are shown in figures 5 and 6 for $\beta = 0{\cdot}5$ and 1; the vortex centre locations are given in table 2. These graphs can be directly compared with the flow fields for solid plugs shown in figures 2 and 3. As would be expected, fluid flow rates are greater near the plane boundaries of the cavity when gas plugs are used, and the stream function increases more

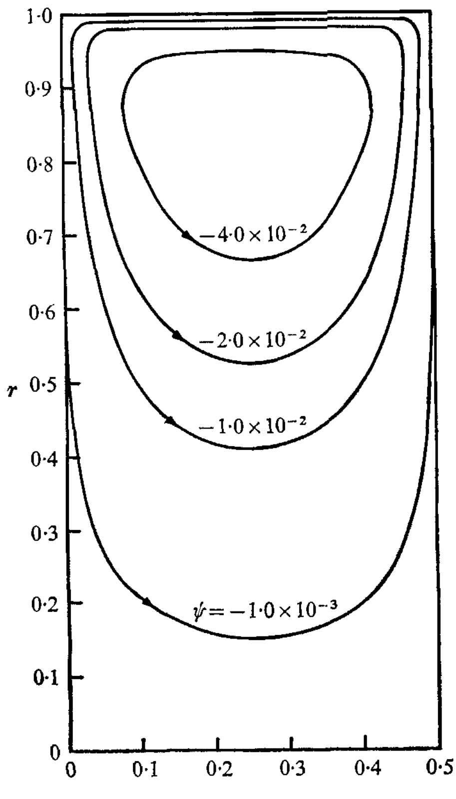

FIGURE 5. Streamline pattern for $\beta = 0{\cdot}5$ with no drag boundary condition.

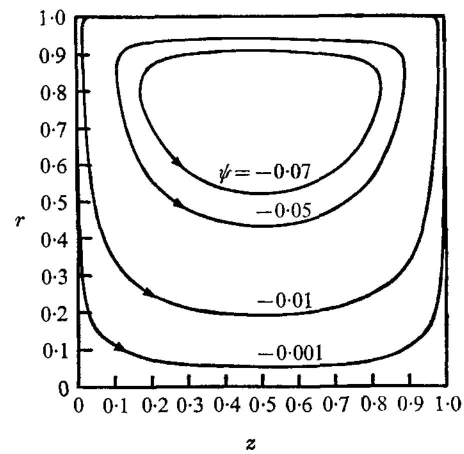

FIGURE 6. Streamline pattern for $\beta = 1$ with no drag boundary condition.

rapidly near these boundaries. In addition, the two-cell circulation pattern observed for $\beta = 0{\cdot}5$ for solid plugs is not in evidence for the gas plugs because the resistance of the plugs to flow has effectively disappeared. The velocity field in a fluid which circulates between plugs with a consistency somewhere between the solid and gas plugs can of course be visualized as being intermediate to the cases considered here.

Appendix

$$g_m = J_0^2(a_m)\,[4a_m^2\beta\, e^{a_m\beta} + (2e^{a_m\beta}/\beta) - (e^{-a_m\beta}/\beta) - (e^{3a_m\beta}/\beta)],$$

$$T_{mnp} = \frac{R_{mp}Q_{np}[-4a_p\beta\, e^{a_p\beta} + 2(-1)^n(1-e^{2a_p\beta})]}{g_p} + \frac{S_{mp}Q_{np}[4a_p\, e^{a_p\beta} - (2e^{a_p\beta}/\beta) + (2e^{-a_p\beta}/\beta)]}{g_p} - \frac{S_{mp}Q_{np}(-1)^n[4a_p + (2/\beta) - (2e^{2a_p\beta}/\beta)]}{g_p}.$$

$$c_m = \frac{\beta[1-(-1)^m]}{m\pi},$$

$$a_m = \tfrac{1}{2}m\pi\left[\frac{I_0(m\pi/\beta)\,I_2(m\pi/\beta)-I_1^2(m\pi/\beta)}{I_2^2(m\pi/\beta)}\right].$$

$$R_{mp} = \frac{2m\pi a_p^2 J_0(a_p)\,[(-1)^m\,(e^{a_p\beta}-e^{-a_p\beta})+(1-e^{2a_p\beta})]}{\beta^2[(m\pi/\beta)^2+a_p^2]^2},$$

$$S_{mp} = \frac{2m\pi a_p^2 J_0(a_p)\,[2(-1)^m\,e^{a_p\beta}-(1+e^{2a_p\beta})]}{\beta[(m\pi/\beta)^2+a_p^2]^2},$$

$$Q_{np} = \frac{2a_p n^2\pi^2 I_1^2(n\pi/\beta)\,J_2(a_p)}{\beta^2 I_2^2(n\pi/\beta)\,[(n\pi/\beta)^2+a_p^2]^2}.$$

REFERENCES

Bhattacharji, S. & Savic, P. 1965 *Proceedings of Heat Transfer and Fluid Mechanics Institute*. Stanford University Press.

Bugliarello, G. & Hsiao, G. C. C. 1967 *7th International Conf. on Medical and Biological Engineering*.

Burggraf, O. R. 1966 *J. Fluid Mech.* **24**, 113.

Bye, J. A. T. 1966 *J. Fluid Mech.* **26**, 577.

Figueiredo, O. & Charles, M. E. 1968 *Can. J. chem. Engng*, **46**, 62.

Gill, A. E. 1966 *J. Fluid Mech.* **26**, 515.

Johansson, H., Olgard, G. & Jernqvist, A. 1970 *Chem. Engng Sci.* **25**, 365.

Johns, L. E. & Beckmann, R. B. 1966 *A.I.Ch.E.J.* **12**, 10.

Kantorovich, L. V. & Krylov, V. I. 1958 *Approximate Methods of Higher Analysis*. New York: Interscience.

Kronig, R. & Brink, J. C. 1950 *Appl. sci. Res.* A **2**, 142.

Lew, H. S. & Fung, Y. C. 1969 *Biorheology*, **6**, 109.

Lighthill, M. J. 1968 *J. Fluid Mech.* **34**, 113.

Morse, P. M. & Feshbach, H. 1953 *Methods of Theoretical Physics*. New York: McGraw-Hill.

Oliver, D. R. & Wright, S. J. 1964 *British Chem. Engng*, **9**, 590.

Oliver, D. R. & Young Hoon, A. 1968*a* *Trans. Inst. chem. Engng*, **46**, T 106.

Oliver, D. R. & Young Hoon, A. 1968*b* *Trans. Inst. chem. Engng*, **46**, T 116.

Pan, F. & Acrivos, A. 1967 *J. Fluid Mech.* **28**, 643.

Prothero, J. & Burton, A. C. 1961 *Biophys. J.* **1**, 565.

Prothero, J. & Burton, A. C. 1962 *Biophys. J.* **2**, 199.

Taylor, G. I. 1923 *Phil. Trans.* A **223**, 289.

Timoshenko, S. & Woinowsky-Krieger, S. 1959 *Theory of Plates and Shells*. New York: McGraw-Hill.

Wang, H. & Skalak, R. 1969 *J. Fluid Mech.* **38**, 75.

Weiss, R. F. & Florsheim, B. H. 1965 *Phys. Fluids*, **8**, 1631.

Wilkes, J. O. & Churchill, S. W. 1966 *A.I.Ch.E.J.* **12**, 161.

Wingard, L. B. 1969 *Chem. Engng Prog.* **65**, 69.